# 비탄성 강재 부재의 좌굴 해석

## Buckling Analysis of Inelastic Steel Members

길 홍 배[1]

*Gil, Heung-Bae*

요    약 : 본 연구에서는 비탄성 부재들의 좌굴 강도를 결정하기 위한 계산적으로 효율적인 비탄성 좌굴해석 프로그램이 개발되었다. 본 프로그램은 휨 좌굴, 휨-비틈 좌굴 혹은 국부좌굴에 의해 붕괴되는 탄성과 비탄성 부재들의 좌굴 강도 및 형상을 결정할 수 있다. 일축 대칭이나 2축 대칭인 I 형 부재를 해석할 수 있다. 복부판은 판 요소를 이용하여 모델되고, 플랜지는 보 요소로 모델되었다. 재료의 비탄성 응력-변형률 관계를 모사하기 위하여 다선형 등방경화 법칙과 증분이론이 사용되었다. 프로그램은 이론치와 실험값들을 이용하여 입증되었다. 프로그램의 결과는 이론치 및 실험값들과 잘 일치였다.

ABSTRACT : In this study, the computationally efficient inelastic buckling analysis program is developed to be used as the research tool in finding buckling strength of inelastic members. The program can determine buckling loads and buckled shapes of elastic and inelastic members which failed by flexural, lateral-torsional and/or local buckling. It can analyze singly and doubly symmetric I-shape members. In the program, the web of the member is modeled using the plate element and the flanges are modeled by beam elements. Multilinear isotropic hardening rule and the incremental theory of plasticity are used to simulate the inelastic stress-strain relationship from material tests. The program is verified using theoretical solutions and experimental results. The results from the program show good agreement with those from experiments and theory.

핵 심 용 어 : 좌굴, 비탄성, 안정도, 비탄성 좌굴, 소성
KEYWORDS : Buckling, Inelasticity, Stbility, Inelastic Buckling, Plasticity

## 1. Introduction

As the understanding and knowledge of structural members' behavior and mate-rial properties expand, more structural members are loaded to the inelastic range of the material to take full advantage of material strength. The main failure modes of inelastically loaded steel members are

---

1) 한국도로공사 책임연구원

either yielding or buckling. Lateral torsional and local buckling can occur for the I-shaped steel members in the inelastic range.

The finite element method which is derived using the principle of stationary potential energy has been employed tq solve general buckling problems. Kapur and Harts[12] solved the problem of plate stability using the method. Barsoum and Gallagher[4] solved torsional and flexural-torsional buckling of one-dimensional prismatic members. Powel and Klingner[14] employed the finite element method to solve elastic lateral torsional buckling of steel beams. Local and distortional buckling was not considered in their model. Akay, Johnson, and Will[2] developed the two-dimensional elastic buckling analysis program which can find lateral torsional, local, and distortional buckling loads of structural members. El-Ghazaly et al.[7] followed Akay et al's approach and developed the inelastic buckling analysis program. But the program was limited to specific cases. As summarized by Bradford[5], finite element method has been actively adopted by Australian researchers to perform lateral-distortional buckling analysis. Commercial programs like ANSYS, ABAQUS have the capacity for elastic buckling analysis but do not have the routine to determine inelastic buckling loads.

The purpose of the study is to develop the inelastic buckling analysis program, IBASP (Inelastic Buckling Analysis of Stiffened Plate). The developed program can predict the inelastic as well as elastic buckling capacities of the members. Lateral-torsional, local, and distortional buckling capacities of the members can be found. However, the program cannot determine post-buckling strength and the displacement at the instant of and after the instability. It also does not consider initial imperfections of the member. The program can deal with singly- and doubly-symmetric I-shape cross-sections.

## 2. Problem Statement

The linear buckling equation is obtained from the second variation of the potential energy and expressed as

$$([K] + \lambda_{cr}[K_G])\{\partial D\} = \{0\} \qquad (1)$$

where $[K]$ is the conventional stiffness matrix, $[K_G]$ is the geometric stiffness matrix, $\lambda_{cr}$ is the lowest eigenvalue, and $\{\partial D\}$ is the infinitesimal displacement
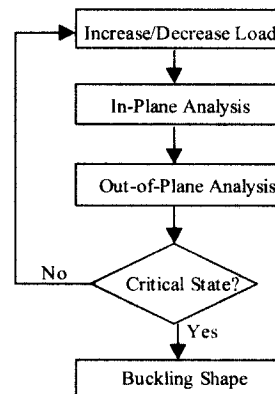


Fig. 1 Schematic Flowchart of Computational Procedure

vector. The conventional stiffness matrix, $[K]$, depends on the state of material in the inelastic range. The geometric stiffness matrix $[K_G]$ is the function of membrane stresses that are present in the element prior to buckling. Eq. 1 is characterized as the standard eigenvalue problem whose eigenvalues are buckling load multipliers. In a buckling problem, the lowest eigenvalue and eigenvector which represent lowest buckling load and a corresponding mode shape are usually of the greater interest. This load is defined as bifurcation buckling load which may not be the true collapse load of a member. The collapse load can be quite different from the buckling load because of post-buckling strength.

The computational process of the finite element program is composed of three main parts as schematically shown in Fig. 1. In the first part, in-plane stress analysis is performed to determine the distribution of the membrane stresses and the state of the material under applied loads. It is followed by out-of-plane stiffness analysis. In the second part, conventional and geometric stiffness matrices, $[K]$ and $[K_G]$, are assembled. Last, the buckling load and the mode shape are determined. The inverse iteration method with shift is employed to define the buckled shape.

In the program, elements which can accommodate inelastic deformation are employed. The web of a I-shape member is modeled using the isoparametric plane stress elements for in-plane stress analysis and the degenerated isoparametric plate elements for out-of-plane behavior. Each node of the isoparametric element shown in Fig. 2 has five degrees of freedom. Two degrees of freedom are for the in-plane analysis and remaining three are for out-of-plane analysis. The flange of a member is modeled using beam elements. Akay, Johnson, and Will[2] observed that modeling of flanges and stiffeners using beam elements resulted in substantial reduction in computation time and no significant loss in accuracy. For the new program, flanges and stiffeners of the member are modeled using the layered beam elements by Owen and Hinton[13]. The layered beam element shown in Fig. 3 can account for the spread of inelasticity through the depth of the beam.

The tangent modulus theory has been used to predict the buckling capacities of inelastic members. The theory which is experimentally proven by Shanley[15] states that the buckling capacity of the inelastic member is the function of tangent modulus rather than reduced modulus of the material. In the program, the tangent modulus theory is adopted to determine inelastic buckling capacities. When the material is stressed over the yield strength of the material, tangent modulus is used in the formation of stiffness matrices. The detailed description of the computational process of IBASP is given below.

# 3. In-Plane Stress Analysis

The in-plane stress analysis routine determines membrane stresses and the state of the material. In the routine, the web of the member is modeled using isoparametric plane stress elements and flanges and stiffeners of the member are modeled using the layered beam elements with the axial degree of freedom only. When the material is in the inelastic state, an iterative solution method, a modified Newton-Raphson method, is used to solve non-linear problems due to inelasticity. The plasticity algorithm which determines the state of material and forms the tangent stiffness matrix is required to solve plasticity problems. The elastic predictor-radial return algorithm





Fig. 2 Nine Node Isoparmetric Plate Elements

recommended by Dodds[6] is adopted in the study.

## 3.1 Web Element

The nine-node isoparametric plane stress element shown in Fig. 2 is selected because the isoparametric element can accommodate inelastic deformation. Numerical integration methods are used to form the stiffness matrix because of its convenience and easy implementation. Stresses at numeral integration points of the elements are saved to keep track of the state of material.

If the state of the material is elastic, the elastic stiffness matrix is formed and stresses are calculated. When applied stresses exceed the yield strength of a material, plasticity theories are needed to describe the behavior of the material and form the stiffness matrix. In this study, the incremental theory of plasticity is employed. The theory relates the increment of plastic strain to the increment of stresses and depends on stress history. The details of the theory are discussed below.
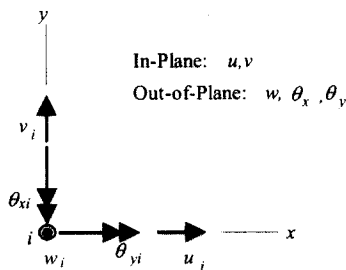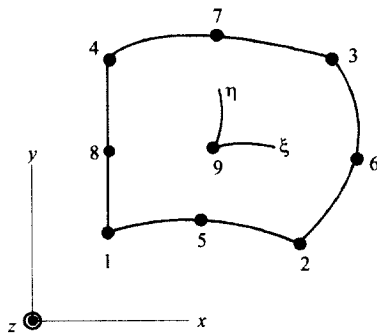
## 3.2 Incremental Theory of Plasticity

This theory relates the plastic strain rate to the rate of yield criterion. The three components of the incremental theory of plasticity are a yield surface, a flow rule, and a hardening rule. The yield surface is defined as the shape of yield function in the stress plane. The von

Mises yield criterion which well represent the behavior of steel is adopted in this study. The flow rule determines the direction of plastic strain. The associated flow rule which states that the direction of plastic flow is normal to the yield surface is employed here. The hardening rule describes the behavior of strain hardening materials. The multi-linear isotropic hardening rule is employed here. According to Hunsaker[11], the isotropic hardening rule is simple to use and takes the least amount of computer storage for the loading history without unloading or load reversal.

In multi-axial states of stresses, effective stress and effective strain are used to describe the behavior of the material. The effective stress, $\sigma_e$, and effective strain, $\varepsilon_e$, for plane stress are defined as

$$\sigma_e = \sqrt{(\sigma_x^2 + \sigma_y^2 - \sigma_x \sigma_y + 3\tau_{xy}^2)} \qquad (2)$$

$$\varepsilon_e = \frac{2}{\sqrt{3}} \sqrt{\left(\varepsilon_x^2 + \varepsilon_y^2 + \varepsilon_x \varepsilon_y + \frac{\gamma_{xy}^2}{4}\right)} \qquad (3)$$

where $\sigma_i$ = membrane stresses; $\varepsilon_i$ = membrane strains. The effective strain in the inelastic state is composed of elastic strain component ($\varepsilon_e^e$) and plastic strain component ($\varepsilon_e^p$).

The tangent modulus, $E_T$, in the inelastic range is defined in terms of effective stress and effective strain and given by

$$E_T = \frac{d\sigma_e}{d\varepsilon_e} = \frac{d\sigma_e}{d\varepsilon_e^e + d\varepsilon_e^p} = \frac{d\sigma_e}{d\sigma_e/E + d\varepsilon_e^p} \qquad (4)$$

where $E$ = elastic modulus; $d\sigma_e$ = effective stress variation; $d\varepsilon_e$ = effective strain variation; $d\varepsilon_e^e$ = elastic effective strain variation; $d\varepsilon_p^e$ = plastic effective strain variation. Eq. 4 yields the plastic modulus $E_P$ which relates stress variation to plastic strain variation as follows:

$$\frac{d\sigma_e}{d\varepsilon_e^p} = E_P = \frac{E E_T}{E - E_T} \qquad (5)$$

The elasto-plastic constitutive matrix, $[D_{ep}]$, for the incremental theory is obtained as

$$d\{\sigma\} = [D_{ep}]d\{\varepsilon\} = ([D_e] - [D_p])d\{\varepsilon\} \qquad (6)$$

where $[D_e]$ is the elastic constitutive matrix and $[D_p]$ is the plastic constitutive matrix which is defined as

$$[D_p] = \frac{[D_e]\frac{\partial \sigma_e}{\partial \{\sigma\}} \left\{\frac{\partial \sigma_e}{\partial \{\sigma\}}\right\}^T [D_e]}{E_p + \left\{\frac{\partial \sigma_e}{\partial \{\sigma\}}\right\}^T [D_e]\frac{\partial \sigma_e}{\partial \{\sigma\}}} \qquad (7)$$

The elasto-plastic stiffness matrix, $[D_{ep}]$, is used in the in-plane stress analysis routine and in the derivation of the out-of-plane plate stiffness matrix.

### 3.3 Flange Element

In the program IBASP, the layered

beam element by Owen and Hinton[13] is used to model flanges and stiffeners. As shown in Fig. 3, the cross-section of the beam is subdivided into $N$ layers. The advantage of the layered beam element is that it can follow the spread of inelasticity through the depth of the beam by assessing the state of the material at each layer during in-plane and out-of-plane analysis. The axial stiffness of the layered beam, $EA$, is the summation of the axial stiffness from each layer and defined as follows:

$$EA = \sum_{l=1}^{N} E_l \, b_l \, t_f \qquad (8)$$

where $E_l$ is the modulus of a layer, $b_l$ is the width of a layer, and $t_f$ is the thickness of the beam element.

When plastic deformation occurs, the



(a) cross-section of the layered beam
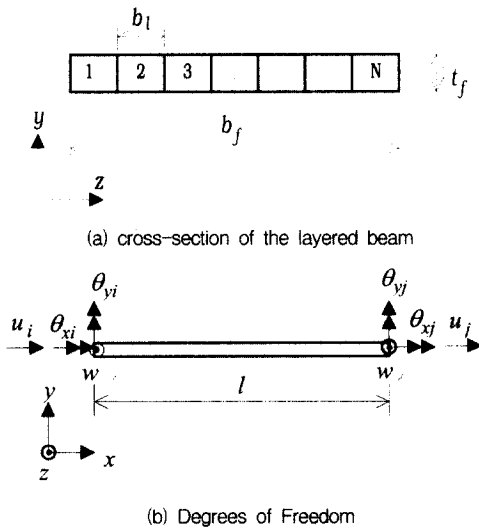


(b) Degrees of Freedom

Fig. 3 Layered Beam Element

spread of plasticity is monitored at each layer. It is assumed that the layer becomes inelastic when the middle of the layer reaches the yield strength of the material. The incremental inelastic stress-strain relationship of the layered beam is now defined. The total strain increment in the inelastic range is composed of elastic and plastic components as follows:

$$d\varepsilon = d\varepsilon^e + d\varepsilon^p \qquad (9)$$

Then, the increment of stress in the plastic range is defined as:

$$d\sigma = Ed\varepsilon^e = E(d\varepsilon - d\varepsilon^p) \qquad (10)$$

The plastic strain increment $d\varepsilon^p$ is derived from Eq. 5 as $d\varepsilon^p = d\sigma/E_p$ and substituted into Eq. 12. Then, the elasto-plastic stiffness $E_{ep}$ can be derived as

$$E_{ep} = \frac{d\sigma}{d\varepsilon} = \frac{E E_p}{E + E_p} \qquad (11)$$

The elasto-plastic stiffness is used in the derivation of the axial and bending stiffnesses of the yielded layer.

## 4. Out-of-Plane Analysis

In the out-of-plane analysis routine, the out-of-plane stiffness matrix and the geometric stiffness matrix are formed. If the material state is over the yield limit,

the out-of-plane stiffness matrix using the tangent modulus is assembled.

## 4.1 Web Element

The degenerated isoparametric shell element which is developed by Ahmad et al.[1] is employed. The element is based on the Mindlin plate theory which allows transverse shear deformations so that a line that is straight and normal to the midsurface before loading is assumed to remain straight but not normal to the midsurface. The advantage of the isoparametric shell element is that the shape functions from plane stress elements can be used again for plate bending element. It can also accommodate the spread of inelasticity. Each node of the shell element shown in Fig. 1 has three out-of-plane independent degrees of freedom: one translation, $w$, and two rotations, $\theta_x$ and $\theta_y$.

The element stiffness matrix $[K]$ of the element can be divided into two matrices: a bending stiffness matrix $[K_b]$ and a shear stiffness matrix $[K_s]$. The bending stiffness matrix contains terms related only with plate bending stiffness while the shear stiffness matrix is only associated with transverse shear stiffness. As for the plane stress element, a numerical integration technique is used to obtain the stiffness matrices. For a nine-node isoparametric shell element, a 3×3 (nine) mesh of Gauss integration points is needed for full numerical integration.

## 4.2 Beam Element

The bending and torsional stiffness matrices of the beam elements are needed for buckling analysis. The degrees of freedom $w$ and $\theta_y$ in Fig. 2 are related to the flexural behavior of the beam element in the out-of-plane direction and the degree of freedom $\theta_x$ represents the torsion of the beam element. The bending stiffness, $EI$, and torsional stiffness $GJ$, of the layered beam are calculated as:

$$EI = \sum_{l=1}^{N} ( E_l \, b_l \, t_f z_l^2 + E_l \, t_f b_l^3/12) \quad (12)$$

$$GJ = \sum_{l=1}^{N} G_l \, b_l t_f^3/3 \quad (13)$$

where $G_l$ is the shear modulus of the layer and $z_l$ is the $z$-coordinate at the middle of the layer. It was assumed that the inelastic shear modulus is the same as the elastic one.

## 4.3 Geometric Stiffness

The geometric stiffness matrix of plate elements is formed using membrane stresses from the prior in-plane analysis routine. Membrane forces which are a summation of membrane stresses through the thickness $t$ are defined as

$$N_x = \int_{-t/2}^{t/2} \sigma_x dz, \qquad N_y = \int_{-t/2}^{t/2} \sigma_y dz,$$

$$N_{xy} = \int_{-t/2}^{t/2} \tau_{xy} dz \quad (14)$$

where $N_i$ and $\sigma_i$ represent membrane forces and stress, respectively. Then, the geometric stiffness matrix $[K_G]$ for the plate element is defined as

$$[K_G] = \int \int [G]^T \begin{bmatrix} N_x & N_{xy} \\ N_{xy} & N_y \end{bmatrix} [G] \ dxdy \tag{15}$$

where the matrix $[G]$ is obtained from a small rotation-displacement relationship. The matrix is obtained from

$$\begin{Bmatrix} w_{,x} \\ w_{,y} \end{Bmatrix} = [G]\{d_o\} \tag{16}$$

in which $\{d_o\}$ is the out-of-plane displacement vector, $\{w \ \theta_x \ \theta_y\}$. In the derivation of the geometric stiffness matrix, the out-of-plane displacement, $w$, and membrane forces, $N_x$, $N_y$, and $N_{xy}$, are assumed to be independent of each other.

The geometric stiffness matrix of the beam element, $[K_G^b]$, depends on the axial load and the length of the element. The matrix is defined as follows:

$$[K_G^b] = \frac{P}{l} \begin{bmatrix} 1 & -1 \\ -1 & 1 \end{bmatrix} \tag{17}$$

where $l$ is the length of the element and $P$ represents the axial load. The axial load of the layered beam element is obtained using $P = \sum_{l=1}^{N} \sigma_l \ b_l \ t_f$ where $\sigma_l$ is axial stress of each layer. Degrees of freedom associated with $[K_G^b]$ are out-of-plane displacements, $w_i$ and $w_j$.

## 5. Buckling Load and Programming

### 5.1 Buckling Load and Shape

Because the buckling equation given in Eq. 1 is considered as a standard eigenproblem, eigenproblem solution methods are used to determine buckling loads. Iteration methods are generally preferred for solving large size eigenproblems. The nontrivial solution of Eq. 1 exists only if the determinant of stiffness matrices summation is equal to zero. The determinant is expressed as follows:

$$|[K] + \lambda[K_G]| = 0 \tag{18}$$

For the given state of stress, the eigenvalue $\lambda$ assumes certain values to satisfy the above equation. When the critical (buckling) state of stresses is reached, the eigenvalue $\lambda$ should be equal to $1.0$[9]. Thus, it can be stated that buckling happens when $\lambda = 1.0$.

A Sturm sequence property[9] is used to determine whether or not the critical state is reached. This property states that the number of changes in signs of leading principal minors of a standard eigenproblem like $([A] - \lambda[B])$ is equal to the number of eigenvalues less than the current $\lambda$. Leading principle minors are obtained by factorizing the matrix. The matrix $([K] + \lambda[K_G])$ is factorized into

$[L][D][L]^T$ where $[L]$ is the lower triangular matrix and $[D]$ is the diagonal matrix: $[D] = d_{ii}[I]$ where $[I]$ is the identity matrix. The diagonal elements of the matrix $[D]$ represent leading principal minors. The Sturm sequence property can be restated as the number of negative elements in $[D]$ equals to the number of eigenvalues smaller than $\lambda$. When the critical state $\lambda = 1.0$ is reached, a slight increase of $\lambda$, say $\lambda + \alpha$, results in *one* negative element in the matrix $[D]$. The slight decrease of $\lambda$, $\lambda - \alpha$, will lead all positive elements in $[D]$. $\alpha$ represents the solution tolerance and can be changed. By using the Sturm sequence property, the buckling load can be determined by just looking at the leading principal minors of the matrix rather than calculating eigenvectors as well as eigenvalues to see whether $\lambda = 1.0$ is reached or not. After finding the buckling load, a corresponding buckling shape is determined using the subspace iteration method with shifts[10]. A few iterations would be enough to find the buckled shape when the true critical state is reached.

### 5.2 Residual Stress

Residual stress generated from different cooling rates on different parts of a cross-section reduce the buckling capacities of inelastic beams and columns. Compressive residual stress occurs at more exposed areas like flange tips for rolled I-shaped sections. The junction of flanges and a web in I-shaped sections cools later and has tensile residual stresses. The residual stress model by Galambos and Ketter[8] has been widely used and is employed in the program. In the IBASP, a user can decide whether residual stresses need to be included or not.

### 5.3 IBASP Programming and Limit

IBASP which run on a personal computer was programmed using FORTRAN 77 and compiled using a WATCOM FORTRAN 77[32] compiler[7]. The graphic routines from the compiler were also used to draw a buckled shape. The number of elements and nodes allowed in IBASP is 40 nine-node elements and 200 nodes but can be extended depending on computer capacity. The 200 beam elements used to model the stiffeners and flanges are allowed in IBASP.

## 6. IBASP Validation

Theoretical buckling solutions and test results are adopted to calibrate the IBASP program. The buckling moments of simply supported beams are determined using IBASP. The cross-section shown in Fig. 4



$d = $ 304.8 mm (12.0")
$b = $ 304.8 mm (12.0")
$t_w = $ 12.7 mm (0.5")
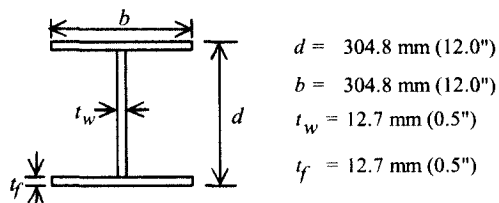$t_f = $ 12.7 mm (0.5")
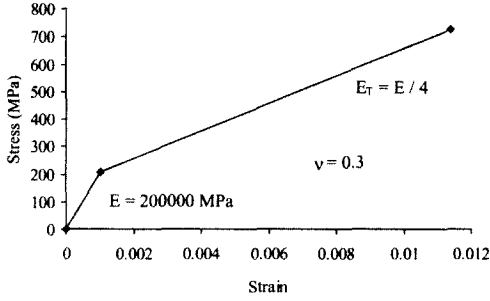
Fig. 4 Cross-section Properties

Fig. 5 Assumed Material Properties



Fig. 6 Simply Supported Beam Model

was assumed for the beam. The buckling capacity of the inelastic member depends on tangent modulus so that an idealized bilinear stress-strain relationship with constant tangent modulus in the inelastic region was assumed and shown in Fig. 5. The results from Bansal's continuous beam tests[3] are used where the beams were failed by lateral buckling. The local buckling prediction capacity of the IBASP was measured using Elgaaly and Salkar's test results[19].

## 6.1 Simply Supported Beam with Constant Moment

The simply supported beam under a constant moment as shown in Fig. 6 is used to compare the results from the IBASP to the theoretical solutions by Timoshenko and Gere[16]. The elastic buckling moment, $M_{cr}^{E}$, is expressed as

$$M_{cr}^{E} = \frac{\pi}{l}\sqrt{E\,I_{y}(GJ + E\,C_{w}\frac{\pi^{2}}{l^{2}})} \qquad (19)$$

Timoshenko and Gere (1961) suggested that the inelastic buckling moment is obtained by multiplying the inelasticity ratio, $\tau$, to the above equation. Then, the inelastic buckling moment, $M_{cr}^{I}$, is expressed as follows,

$$M_{cr}^{I} = \tau M_{cr}^{E} \qquad (20)$$

However, the inelastic buckling moment of Eq. 20 is reported to be too conservative because the shear modulus is assumed to be reduced in the inelastic range[18]. If the elastic shear modulus is used as the inelastic shear modulus, the inelastic buckling moment becomes

$$M_{cr}^{I} = \frac{\pi}{l}\sqrt{E_{T}\,I_{y}(GJ + E_{T}\,C_{w}\frac{\pi^{2}}{l^{2}})} \qquad (21)$$

The analysis results along with the theoretical solutions are plotted in Fig. 7. It shows the relationship between the
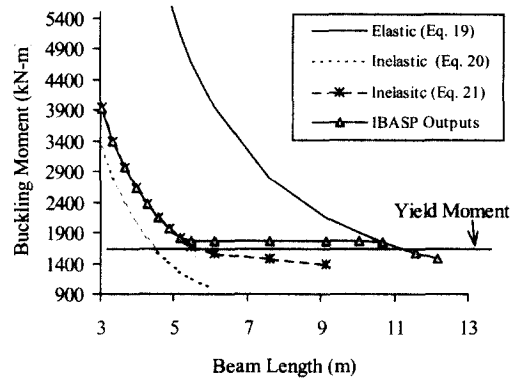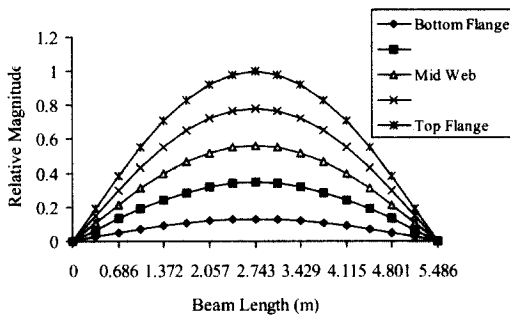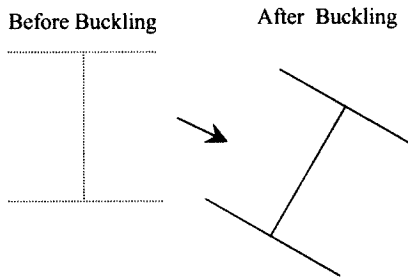


Fig. 7 Buckling Moments of the Beam

lateral-torsional buckling moments and the beam lengths. In the inelastic range, the inelastic buckling moments from Eq. 21 closely match with those from the IBASP using the incremental theory of plasticity. The buckled shape and cross-section deformation are shown in Fig. 8.



(a) Lateral-Torsional Buckling Shape



(b) Buckled Shape at Midspan

Fig. 8 Buckling Shape of Simply Supported Beam

## 6.3 Bansal's Test

Bansal[3] conducted a total of 37 buckling tests using three span continuous steel beams to study elastic and inelastic instability behavior. Rolled I-shaped beams and plate girders were used in tests. The results from the test No. 6 which failed by inelastic lateral buckling are used here to compare with those from the program, IBASP.

Test setups and dimension of the beam are illustrated in Fig. 9. The load was applied at the center of the beam which was braced for the out-of-plane displacement at the supports and the loading point. The cross-section dimensions of the beam are as follows: depth of the section= 307.3mm, flange width=102.6mm, flange thickness=6.9mm, and web thickness= 5.8mm. The yield strength of the beam was 333 MPa and no strain hardening was reported.

A total of 32 elements (2×16) was used to model the continuous beam. The load vs. the vertical displacement at the midspan curves from experiments and analysis without residual stress is shown in Fig. 10(a). The *lateral buckling load* in the figure represents the observed lateral buckling loads from the experiments. The buckled shape in Fig. 10(b) means that the beam buckled between the braces. The load vs. displacement curve also show that the buckled beam had some post buckling strength. However, as explained earlier, the IBASP can predict the
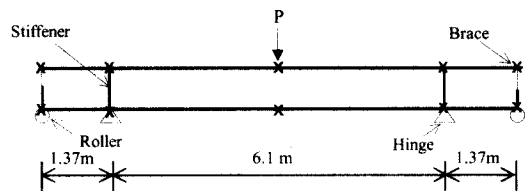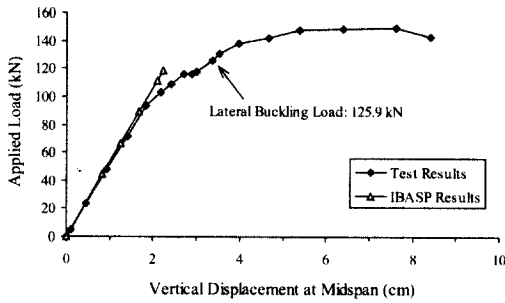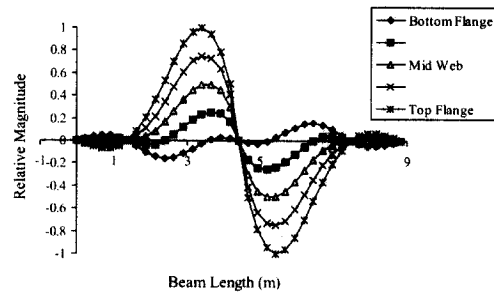


Fig. 9 Bansal 's Test specimen and setup

(a) Load vs Displacement



(b) Buckled Shape

Fig. 10 Bansal 's Test Number 6

buckling load of the beams but not the post buckling strength.

The lateral buckling load from the test was 125.9 kN while the IBASP predicted the buckling load as 118.4 kN when residual stress option was not used. The difference between them is less than 6%. When residual stress option was used with the maximum compressive residual stress of 111 MPa(=yield strength/3) at the tip of the flanges, the buckling load was reduced to 104.5 kN. The compressive residual stress reduces the inelastic buckling strength which depends on the level of compressive stress in the member.
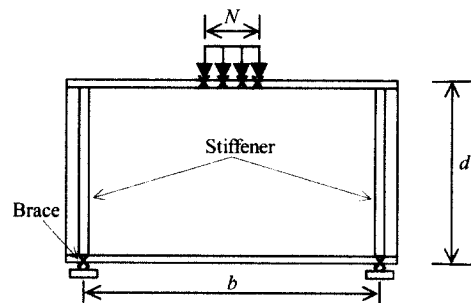
## 6.4 Elgaaly and Salkar's Test

Elgaaly and Salkar[19] performed a series of tests to study local web yielding and buckling behavior of I-shaped beams under in-plane edge loads. Tests were performed on short beams with a concentrated load at the midspan. The result from a test were compared with that from IBASP to see whether IBASP can predict local buckling loads.

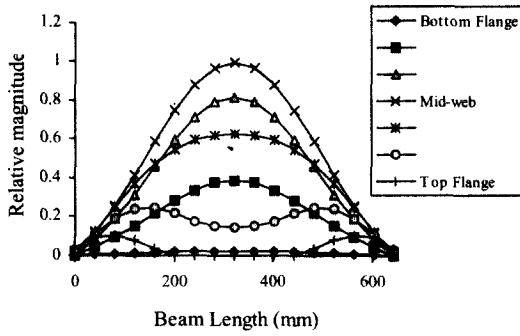The stress-strain relationship of Fig. 11
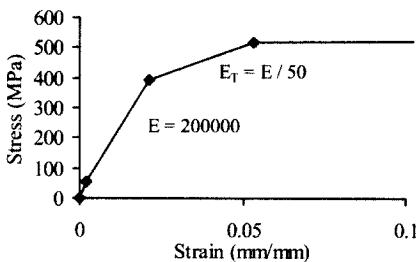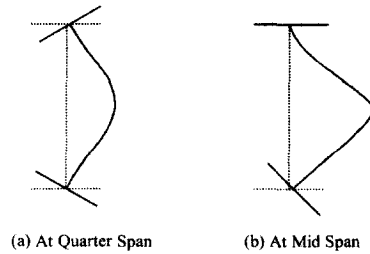


(a) stress-strain relationship



(b) Test Setup

Fig. 11 Stress-Strain Relationship and Test Setup for Elgaaly and Salkar's

(a) Buckled Shape



(a) At Quarter Span    (b) At Mid Span

(b) Cross-section View of Buckled Beam

Fig. 12 Buckled Shape

was used as material data. The yield strength of the material was reported[19], but the strain hardening strain and modulus were assumed for the analysis. Fig. 11(b) shows the test setup. The length of the beam between the supports, $b$ in Fig. 11(b), was 643.6 mm. The measured cross-section dimensions of a W16x31 section are as follows: thickness of flanges=10.92mm, width of flanges= 139.7mm, thickness of web=6.71mm, and depth of section= 404.87mm. During experiments, the ratios of the length of applied load ($N$) to the web depth ($d$), $N/d$, were varied from 0.2 to 0.6. For the comparison, the ratio $N/d$ = 0.4 was used. The beam was braced against out-of-plane displacements and rotations at supports and at the applied load points.

A total of 24 (3×8) nine-node elements were used to model the beam. The buckling load from the test was 652.5 kN while that from the analysis was 700.65 kN. The analytical buckling load was 7%

greater than the experimental buckling load. This may be due to the fact that the stress-strain relationship after yielding is assumed for the analytical study because a complete stress-strain relationship was not reported.

The buckled shape is given in Fig. 12(a). The cross-section of the buckled beam at the quarter span and the mid-span is shown in Fig. 12(b). The buckled cross-section shape indicates that the local distortional buckling occurred rather than the lateral-torsional buckling. It also demonstrates the capacity of the IBASP to predict the distortional buckling as well as the lateral torsional buckling.

## 7. Conclusion

The inelastic buckling analysis program, IBASP, using the finite element method was developed to predict inelastic buck-ling loads of braced and unbraced members. The program can find lateral-torsional, flexural, and local buckling

loads. The theoretical solutions and experimental results were used to test the accuracy of the program. When the results from the program were compared with theoretical and experimental buckling load, not much difference was observed. The IBASP will be a good tool to determine the buckling capacities of inelastic members.

# References

(1) Ahmad, S., Irons, B. M., and Zienkiwicz, O. C., "Analysis of Thick and Thin Shell Structures by Curved Finite Elements," International Journal for Numerical Methods in Engineering, Vol. 3, 1970, pp. 419- 451

(2) Akay, H. U., Johnson, P., and Will, K.M., "Lateral and Local Buckling of Beams and Frames," ASCE, Journal of Structural Divisioin, ST. 9, 1977

(3) Bansal, J. P., "The Lateral Instability of Continuous Steel Beams," Dept. of Civil Engg., Structural Research Laboratory, The University of Texas at Austin, 1971

(4) Barsoum, R. S. and Gallagher, R. H., "Finite Element Analysis of Torsional and Torsional-Flexural Stability Problems," International Journal of Numerical Methods in Engineering, Vol. 2, 1970, pp. 335-352

(5) Bradford, M. A., "Lateral-Distorsional Buckling of Steel I-Section Members," Journal of Constructional Steel Research, Vol. 23, 1992, pp. 97-116

(6) Dodds, R. H., "Numerical Techniques for Plasticity Compuatations in Finite Element Analysis," Compputers & Structues, Vol. 26, No. 5, 1986, pp. 767-779

(7) El-Ghazaly, H. A., Sherbourne, A. N., and Dubey, R. N., "Inelastic Interactive Distorsional Buckling of W-Shape Steel Beams," Computers and Structures, Vol. 19, No. 3, 1984, pp. 351-368

(8) Galambos, T. V. and Ketter R. L., "Columns Uner Combined Bending and Thrust," ASCE, Journal of Engineering Mechanics Division, Vol. 85, 1959

(9) Gupta, K. K., "On a Numerical Solution of the Plastic Buckling Problem of Structures," International Journal for Numerical Methods in Engineering, Vol. 12, 1978, pp. 941-947

(10) Humar, J. L., "Dynamics of Structures," Prentice Hall, Englewood Cliffs, NJ, 1990

(11) Hunsaker, B., "An Evaluation of Four Hardening Rules of the Incremental Theory of Plasticity," Master Thesis, Texas A&M University, 1973

(12) Kapur, K. K. and Hartz, B.J., "Stability of Plates Using the Finite Element Method," ASCE, Journal of Engineering Mechanics Division, Vol.92, No. EM2, April, 1966

(13) Owen, D. R. J. and Hinton, E., "Finite Elements in Plasticity: Theory and Practice," Pineridge Press Limited, Swansea, U.K., 1980

(14) Powel, G. M. and Klingner, R., "Elastic Lateral Buckling of Steel Beams," ASCE, Journal of the Structural Division, Vol. 96, No. ST9, 1970, pp. 1919-1932

(15) Shanley, F. R., "The Colunm Paradox," Journal of Aeronautical Science, Vol. 13, No. 5, 1946, pp. 678

(16) Timoshenko, S. P. and Gere, J. M., "Theory of Elastic Stability," McGraw-Hill Book Company, Inc., New York, 1961

(17) WATCOM FORTRAN 77[32] User's Guide 4th Ed., WATCOM Interna-

tional Corporation, Ontario, Canada, 1993

(18) Galambos,, T. V., "Inelasitc Lateral Buckling of Beams," ASCE, Journal of the Structural Division, Vo. 89, No. ST5, October, pp. 217-242, 1963

(19) Elgaaly, M. and Salkar, R., "Behavior of Webs of Rolled Sections under In-plane Compressive Edge Loads," Department of Civil Engineering, University of Maine, 1990